Exactly solvable two-state quantum model for a pulse of hyperbolic-tangent shape

Lachezar S. Simeonov and Nikolay V. Vitanov
Department of Physics, St. Kliment Ohridski University of Sofia, 5 James Bourchier Boulevard, 1164 Sofia, Bulgaria

(Received 3 February 2014; published 14 April 2014)

We present an analytically exactly solvable two-state quantum model, in which the coupling has a hyperbolic-tangent temporal shape and the frequency detuning is constant. The exact solution is expressed in terms of associated Legendre functions. An interesting feature of this model is that the excitation probability does not vanish, except for zero pulse area or zero detuning; this feature is attributed to the asymmetric pulse shape. Two limiting cases are considered. When the coupling rises very slowly, it is nearly linear and the tanh model reduces to the shark model introduced earlier. When the coupling rises very quickly, the tanh model reduces to the Rabi model, which assumes a rectangular pulse shape and hence a sudden switch on. Because of its practical significance, we have elaborated the asymptotics of the solution in the Rabi limit, and we have derived the next terms in the asymptotic expansion, which deliver the corrections to the amplitude and the phase of the Rabi oscillations due to the finite rise time of the coupling.

DOI: 10.1103/PhysRevA.89.043411 PACS number(s): 32.80.Xx, 32.80.Qk, 33.80.Be, 42.50.Dv

I. INTRODUCTION

It is well known that one can exactly solve the two-state time-dependent Schrödinger equation on resonance, i.e., when the carrier frequency of the external field is equal to the Bohr transition frequency [1]. Several off-resonance two-state models are known that have exact analytical solutions, the most popular of which are the Rabi [2], Landau-Zener-Stückelberg-Majorana [3–6], Rosen-Zener [7], Allen-Eberly [8,9], Bambini-Berman [10], Demkov-Kunike [11–14], Demkov [15], Nikitin [16], and Carrol-Hioe [17] models. All of these except the Rabi model express the respective solution in terms of a special function, which solves a second-order ordinary differential equation: the Weber parabolic cylinder function (Landau-Zener-Stückelberg-Majorana model), the Bessel function (Demkov model), the Gauss hypergeometric function (Rosen-Zener, Allen-Eberly, Bambini-Bermann, Demkov-Kunike, and Carroll-Hioe models), the Kummer confluent hypergeometric function (Nikitin model), etc. A different approach has been used by Barnes and Das Sarma [18], who derived a variety of solvable models by assuming that the solution is known and considered the Schrödinger equation to be an equation for the pulse shape.

In this paper, we introduce an exactly solvable model, in which the Rabi frequency has a hyperbolic-tangent temporal shape; that is, it increases monotonically from zero toward a constant value. This model can be considered a generalization of the rectangular pulse in the Rabi model, to which it reduces in the extreme limit of very fast pulse rise. In the other limit, very slow pulse rise, the tanh model reduces to the linear shark model derived earlier [19]. We derive the exact propagator, which is expressed in terms of associated Legendre functions, and then verify the limits of the Rabi and shark models. We pay special attention to the asymptotics of the solution in the Rabi limit and derive the corrections to the amplitude and the phase of the Rabi oscillations due to the finite rise time of the coupling.

This paper is organized as follows. In Sec. II we define the tanh model and derive the exact propagator. In Sec. III A we explore the limiting case of a very steep turn-on, and we calculate the corrections to the Rabi formula. In Sec. III B we investigate the opposite case of very slow rise of the field, and we derive the shark model limit [19]. Finally, in Sec. IV we give a summary and an outlook.

II. HYPERBOLIC-TANGENT (TANH) MODEL

A. Definition of the tanh model

We begin with the derivation of the exact propagator for the tanh model. Coherent excitation of a two-state quantum system is described by the Schrödinger equation [1]

$$i\hbar\frac{d\mathbf{c}}{dt} = \mathbf{H}\mathbf{c}, \tag{1}$$

where $\mathbf{c}(t) = [c_1(t), c_2(t)]^{\mathrm{T}}$ is a two-dimensional vector comprising the complex probability amplitudes of the two states $|1\rangle$ and $|2\rangle$. The Hamiltonian in the basis formed by these states has the matrix form [1]

$$\mathbf{H} = \frac{\hbar}{2}\begin{bmatrix} -\Delta(t) & \Omega(t) \\ \Omega(t) & \Delta(t) \end{bmatrix}, \tag{2}$$

where $\Omega(t)$ is the Rabi frequency of the coupling. In coherent atomic excitation, $\Omega(t) = -\mathbf{d}\cdot\mathbf{E}/\hbar$, where $\mathbf{d}$ is the transition electric dipole moment and $\mathbf{E}(t)$ is the laser electric-field envelope, while $\Delta = \omega_0 - \omega$ is the frequency detuning between the Bohr transition frequency ω_0 and the laser carrier frequency ω. This Hamiltonian is valid in the rotating-wave approximation (i.e., for $|\Omega| \ll \omega$ and $|\Delta| \ll \omega$) and for completely coherent evolution [1].

In the Rabi model, we have the simplest nontrivial Hamiltonian (i.e., with $\Delta \neq 0$), in which the coupling and the detuning are constant. With the initial condition usually set at $t_{\mathrm{i}} = 0$, the Rabi model physically implies a sudden switching on of the coupling. In many real experimental situations, however, the electric-field envelope does not possess such an ideal shape.

In order to deal with the finite turn-on time of the coupling we introduce the tanh model,

$$\Omega(t) = \begin{cases} 0 & (t < 0,\ t > T), \\ \Omega_0 \tanh(t/\tau) & (0 \leqq t \leqq T), \end{cases} \tag{3a}$$

$$\Delta(t) = \text{const.} \tag{3b}$$

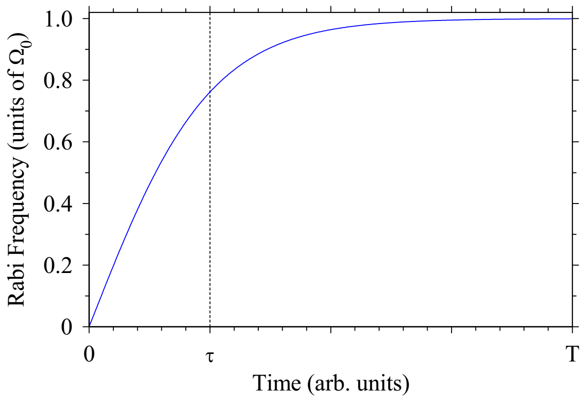

FIG. 1. (Color online) Rabi frequency $\Omega(t) = \Omega_0 \tanh t/\tau$ as a function of time. The duration of the pulse is T.

Here T is the pulse duration and τ is the characteristic rise time of the coupling. This pulse is shown in Fig. 1. The pulse begins at $t_i = 0$, and its amplitude increases monotonically towards the long-time asymptotic value Ω_0. Such a behavior of the amplitude of the driving field is observed, e.g., after a sudden switching on of a rf pulse generator [20]. The pulse area of the tanh pulse is

$$A = \Omega_0 \tau \ln[\cosh(T/\tau)]. \tag{4}$$

Below we derive the propagator for this model and explore the two limits of fast and slow rise of the coupling.

B. Derivation of the propagator

Our objective is to derive the propagator $\mathbf{U}(t,0)$ from time 0 to time t, which is defined as $\mathbf{c}(t) = \mathbf{U}(t,0)\mathbf{c}(0)$. We begin by rotating the state vector at an angle $\pi/4$, $\mathbf{c}(t) = \mathbf{R}(\pi/4)\,\mathbf{b}(t)$, where $\mathbf{R}(\theta)$ is the rotation matrix

$$\mathbf{R}(\theta) = \begin{bmatrix} \cos\theta & -\sin\theta \\ \sin\theta & \cos\theta \end{bmatrix}. \tag{5}$$

The equation for $\mathbf{b}(t)$ reads

$$i\tau \frac{d}{dt}\mathbf{b}(t) = \begin{bmatrix} \alpha \tanh(t/\tau) & \delta \\ \delta & -\alpha \tanh(t/\tau) \end{bmatrix} \mathbf{b}(t), \tag{6}$$

where we have introduced two dimensionless parameters,

$$\alpha = \frac{\Omega_0 \tau}{2}, \qquad \delta = \frac{\Delta \tau}{2}. \tag{7}$$

We assume, without loss of generality, that Ω_0 is positive; hence, because $\tau > 0$, we have $\alpha > 0$. (The phase of Ω_0 can always be attached to the probability amplitudes.) We also assume for simplicity that $\Delta \geqq 0$ because the transition probability does not depend on its sign; hence $\delta \geqq 0$.

A two-state model with the Hamiltonian in Eq. (6) was considered earlier by Demkov and Kunike under the name "second hypergeometric model" [11,14]. Because the coupling in this rotated basis is constant, the transition probability in this model does not converge for initial conditions set at $t \to -\infty$, as considered by Demkov and Kunike [11]; hence they have calculated the probability for nonadiabatic transitions, i.e., the transition probability in the basis of the eigenstates of the Hamiltonian in Eq. (6). Here we have our initial conditions at time $t = 0$, and our pulse in the original basis has a finite duration; hence there are no divergences. Moreover, we are interested in the problem in the original basis (3), which is, of course, very different physically.

We change the independent variable from t to

$$\xi = \tanh\frac{t}{\tau}, \tag{8}$$

which turns Eq. (6) into the equation

$$i(1-\xi^2)\frac{d}{d\xi}\mathbf{b} = \begin{bmatrix} \alpha\xi & \delta \\ \delta & -\alpha\xi \end{bmatrix}\mathbf{b}. \tag{9}$$

Next, we decouple this system of two first-order differential equations. To this end, we express $b_2(\xi)$ from the first equation, substitute it into the second equation of the system (9), and obtain a second-order ordinary differential equation for $b_1(\xi)$,

$$b_1'' - \frac{2\xi}{1-\xi^2}b_1' + \left[\frac{i\alpha(1+i\alpha)}{1-\xi^2} + \frac{\beta^2}{(1-\xi^2)^2}\right]b_1 = 0, \tag{10}$$

where $\beta = \sqrt{\alpha^2+\delta^2}$ and a prime denotes $d/d\xi$. This is the associated Legendre equation, and its solution reads

$$b_1(\xi) = B P_\mu^\nu(\xi) + C Q_\mu^\nu(\xi), \tag{11}$$

where $P_\mu^\nu(\xi)$ and $Q_\mu^\nu(\xi)$ are the associated Legendre functions of the first and second kinds, respectively [21]. Here B and C are integration constants, and

$$\mu = i\alpha, \qquad \nu = i\beta. \tag{12}$$

We find $b_2(\xi)$ by using Eq. (9) and the following properties of the Legendre functions involved [21]:

$$(\xi^2-1)\frac{d}{d\xi}P_\mu^\nu(\xi) = \xi\mu P_\mu^\nu(\xi) - (\mu+\nu)P_{\mu-1}^\nu(\xi), \tag{13a}$$

$$(\xi^2-1)\frac{d}{d\xi}Q_\mu^\nu(\xi) = \xi\mu Q_\mu^\nu(\xi) - (\mu+\nu)Q_{\mu-1}^\nu(\xi). \tag{13b}$$

The solution for $b_2(\xi)$ reads

$$b_2(\xi) = \frac{i(\mu+\nu)}{\delta}\left[B P_{\mu-1}^\nu(\xi) + C Q_{\mu-1}^\nu(\xi)\right]. \tag{14}$$

In order to derive the propagator $\mathbf{V}(t,0)$ in the rotated basis $\mathbf{b}(t)$, defined as $\mathbf{b}(t) = \mathbf{V}(t,0)\mathbf{b}(0)$, we let $\xi \to 0$ in Eqs. (11) and (14) and find

$$B = \frac{1}{D}\left[Q_{\mu-1}^\nu(0)b_1(0) + \frac{i\delta}{\mu+\nu}Q_\mu^\nu(0)b_2(0)\right], \tag{15a}$$

$$C = -\frac{1}{D}\left[P_{\mu-1}^\nu(0)b_1(0) + \frac{i\delta}{\mu+\nu}P_\mu^\nu(0)b_2(0)\right], \tag{15b}$$

with $D = P_\mu^\nu(0)Q_{\mu-1}^\nu(0) - P_{\mu-1}^\nu(0)Q_\mu^\nu(0)$. We find

$$D = \frac{\Gamma(\mu+\nu)}{\Gamma(1+\mu-\nu)}, \tag{16}$$

where we have used the relations

$$P_\mu^\nu(0) = \frac{2^\nu\sqrt{\pi}}{\Gamma\left(\frac{1}{2}-\frac{\mu+\nu}{2}\right)\Gamma\left(1+\frac{\mu-\nu}{2}\right)}, \tag{17a}$$

$$Q_\mu^\nu(0) = -\frac{2^{\nu-1}\pi^{3/2}}{\Gamma\left(\frac{1}{2}-\frac{\mu+\nu}{2}\right)\Gamma\left(1+\frac{\mu-\nu}{2}\right)}\tan\frac{\pi(\mu+\nu)}{2}, \tag{17b}$$

and Eqs. (A4). We substitute Eqs. (15) into Eqs. (11) and (14) and find the propagator elements,

$$V_{11} = \frac{1}{D}\left[P_\mu^\nu(\xi)Q_{\mu-1}^\nu(0) - P_{\mu-1}^\nu(0)Q_\mu^\nu(\xi)\right], \tag{18a}$$

$$V_{12} = \frac{i\delta}{(\mu+\nu)D}\left[P_\mu^\nu(\xi)Q_\mu^\nu(0) - P_\mu^\nu(0)Q_\mu^\nu(\xi)\right], \tag{18b}$$

and $V_{21} = -V_{12}^*$, $V_{22} = V_{11}^*$. The propagator $\mathbf{U}(t,0)$ in the original basis $\mathbf{c}(t)$ is connected to the propagator $\mathbf{V}(t,0)$ in the rotated basis $\mathbf{b}(t)$ via the relation $\mathbf{U}(t,0) = \mathbf{R}(\pi/4)\mathbf{V}(t,0)\mathbf{R}(-\pi/4)$. Explicitly,

$$\mathbf{U}(t,0) = \begin{bmatrix} \mathrm{Re}V_{11} - i\mathrm{Im}V_{12} & \mathrm{Re}V_{12} + i\mathrm{Im}V_{11} \\ -\mathrm{Re}V_{12} + i\mathrm{Im}V_{11} & \mathrm{Re}V_{11} + i\mathrm{Im}V_{12} \end{bmatrix}. \tag{19}$$

Therefore the transition probability is

$$\mathcal{P} = |U_{12}|^2 = (\mathrm{Re}V_{12})^2 + (\mathrm{Im}V_{11})^2. \tag{20}$$

This is the exact solution for the tanh model expressed in terms of associated Legendre functions. Below we shall study the asymptotic behavior of this solution in two limits: (i) fast coupling rise (or long pulse duration), in which the coupling is nearly constant and the tanh model reduces to the Rabi model [2], and (ii) slow coupling rise (or short pulse duration), in which the coupling is nearly linear and the tanh model reduces to the shark model [19].

C. Transition probability

Figure 2 compares the transition probabilities plotted versus the pulse area (4) for the tanh model, Eq. (20), and the Rabi model,

$$\mathcal{P}_{\mathrm{Rabi}} = \frac{\Omega^2}{\Omega^2+\Delta^2}\sin^2\left(\frac{T}{2}\sqrt{\Omega^2+\Delta^2}\right). \tag{21}$$

For small τ and small detuning Δ (top left) the tanh model behaves similar to the Rabi model, and the two curves are barely discernible. A similar conclusion holds for larger τ and small detuning (left column). For large detuning and large τ (bottom right) the tanh model approaches the behavior of the shark model [19], and it behaves very differently from the Rabi model: the transition probability has much lower oscillation amplitude and oscillates around the value $\mathcal{P} = 0.5$. For large detuning and moderate τ (middle right) the tanh model shows a behavior of its own. There are two important features concerning the probability oscillations: the oscillation amplitude in the tanh model decreases compared to the Rabi model, and similarly, a decrease in the oscillation frequency in the tanh model also takes place. Another important difference between the tanh and Rabi models, which is easily visible in the middle and bottom frames of the right column (due to the larger value of τ, which implies a larger deviation from the Rabi model), is that the transition probability for the tanh model does not vanish at any pulse area, except for the trivial value $A = 0$. This is a consequence of the fact that the pulse shape is asymmetric: it is known that for asymmetric pulses the transition probability usually does not vanish [10,19,22], although there are some exceptions [23,24].

The nonvanishing feature of the transition probability is clearly visible in Fig. 3, where the top two frames in the left column of Fig. 2 are plotted in logarithmic scale.

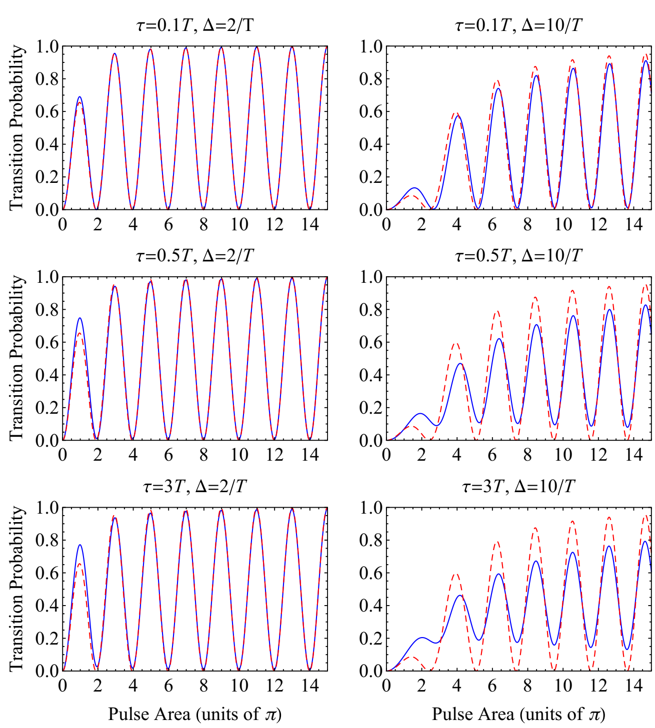

FIG. 2. (Color online) Transition probability vs the pulse area A for various detunings Δ and coupling rise times τ. The values of Δ and τ are given above each frame. Solid curves show the tanh model [Eq. (20)]; dashed curves show the Rabi model [Eq. (29)].

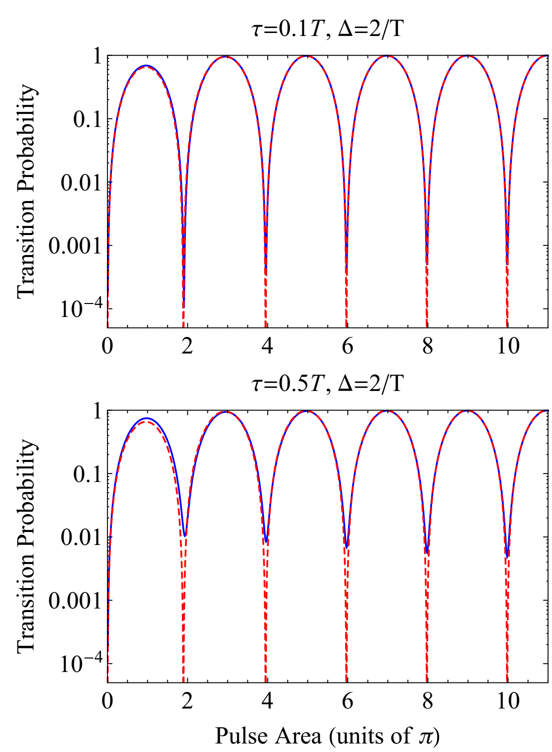

FIG. 3. (Color online) Transition probability in logarithmic scale vs the pulse area A for detuning $\Delta = 2/T$ and two values of the coupling rise time τ, given above each frame. Solid curves show the tanh [Eq. (20)]; dashed curves show the Rabi model [Eq. (29)].

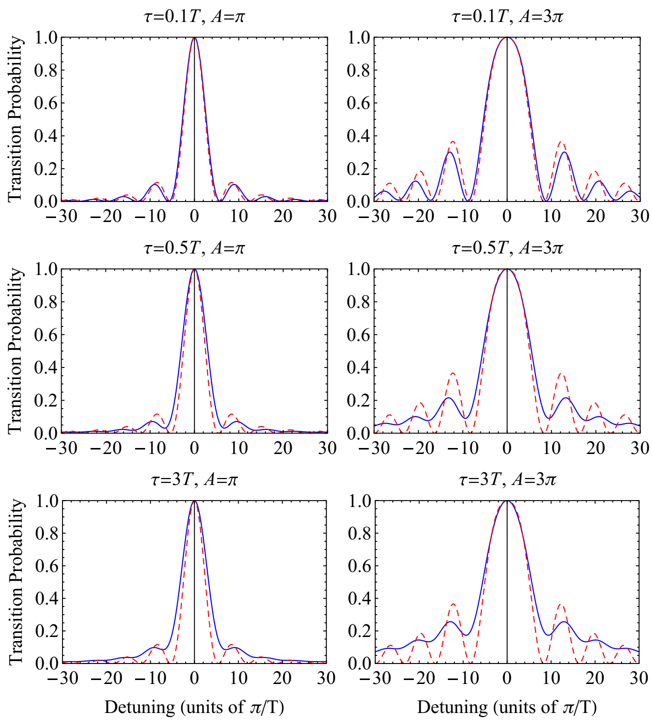

FIG. 4. (Color online) Transition probability vs the detuning for various pulse areas A and coupling rise times τ. The values of A and τ are given above each frame. Solid curves show the tanh model [Eq. (20)]; dashed curves show the Rabi model [Eq. (29)].

The nonvanishing nature of the transition probability is illustrated further in Fig. 4, where it is plotted versus the detuning for pulse areas π and 3π and several values of τ. The power broadening of the excitation profile is evident as the pulse area increases. In all frames the characteristic features of the tanh model compared to the Rabi model are clearly seen: the nonvanishing transition probability, the reduced oscillation amplitude, and the reduced oscillation frequency.

In the next two sections we consider two approximations to the transition probability in two limiting cases. In the limit $\tau \to 0$ (very steep rise) the tanh model reduces to the Rabi model, while in the limit $\tau \to \infty$, the tanh model reduces to the shark model (linear coupling). We pay special attention to the Rabi limit $\tau \to 0$ because of the great importance of the Rabi model in quantum physics. We not only retrieve the Rabi formula in the leading order of the transition probability but also derive the first-order corrections to it, which allow us to explain the observed features in Figs. 2 and 4.

III. LIMITING CASES

A. Fast rise: Rabi model limit

In the limit

$$\tau \to 0, \tag{22}$$

the coupling rises so quickly that the effect of the finite rise time becomes negligible. In this limit, obviously, $\tanh(T/\tau) \approx 1$. To this end, we set

$$\xi = \tanh(T/\tau) = 1 - \epsilon, \tag{23}$$

where $0 < \epsilon \ll 1$. Obviously, $\epsilon \sim 2e^{-2T/\tau}$.

Here it is important to note that when we make the limiting transition (22), we should do so while keeping Ω_0, Δ, and T constant. This means that the dimensionless variables α and δ should also be small,

$$\alpha \to 0, \qquad \delta \to 0. \tag{24}$$

We use the asymptotic expansions of the Legendre functions [21],

$$P_\mu^\nu(1-\epsilon) \sim \frac{(2/\epsilon)^{\nu/2}}{\Gamma(1-\nu)}, \tag{25a}$$

$$Q_\mu^\nu(1-\epsilon) \sim \frac{(\epsilon/2)^{\nu/2}\Gamma(1+\mu+\nu)\Gamma(-\nu)}{2\Gamma(1+\mu-\nu)} + \frac{(2/\epsilon)^{\nu/2}}{2}\Gamma(\nu)\cos\pi\nu, \tag{25b}$$

which are valid in the lowest order in ϵ. Here $\Gamma(z)$ is Euler's gamma function. We substitute these asymptotic expressions into Eqs. (18) and (20), and after simple calculations we obtain the transition probability in the form

$$\mathcal{P} = \frac{\alpha}{\beta}\frac{\sinh(\pi\alpha)}{\sinh(\pi\beta)}\cos\phi\sin^2\frac{\chi}{2} + \frac{\alpha}{2\beta}\sin\phi\sin\chi + \frac{1}{2} - \frac{\delta\sqrt{\sinh^2(\pi\beta)-\sinh^2(\pi\alpha)}+\alpha\sinh(\pi\alpha)}{2\beta\sinh(\pi\beta)}\cos\phi, \tag{26}$$

where

$$\phi = \arg\frac{\Gamma\left(\frac{1}{2}i\alpha+\frac{1}{2}i\beta\right)\Gamma\left(\frac{1}{2}i\alpha-\frac{1}{2}i\beta\right)}{\Gamma\left(\frac{1}{2}+\frac{1}{2}i\alpha-\frac{1}{2}i\beta\right)\Gamma\left(\frac{1}{2}+\frac{1}{2}i\alpha+\frac{1}{2}i\beta\right)}, \tag{27a}$$

$$\chi = \arg\frac{\Gamma(i\alpha+i\beta)\Gamma(i\beta-i\alpha)}{2^{2i\beta}\Gamma^2(i\beta)} + \beta\ln(2\epsilon). \tag{27b}$$

The asymptotics of ϕ and χ in the limit (24) read, up to orders $O(\alpha^3,\alpha^2\beta,\alpha\beta^2,\beta^3)$,

$$\phi \sim 2\alpha\ln 2, \tag{28a}$$

$$\chi \sim \beta\ln\frac{\epsilon}{2}. \tag{28b}$$

Because $\epsilon \ll 1$, we have $\phi \ll 1$ but $\chi \sim O(1)$. Hence we find in the lowest orders of α, β, and δ that

$$\mathcal{P} \sim \frac{\alpha^2}{\beta^2}\sin^2\left(\frac{\beta}{2}\ln\frac{1}{\epsilon}\right). \tag{29}$$

Because $\ln(1/\epsilon) \sim 2T/\tau$, we recover the Rabi formula, Eq. (21), which should be the case in the limit (22).

In order to find the corrections to the Rabi formula, we keep the next terms in α, β, and δ in the expansions above. Thereby we find

$$\mathcal{P} \sim \frac{\alpha^2}{\beta^2}(1-\varkappa_1)\sin^2\left(\frac{\beta}{2}\ln\frac{1}{\epsilon}-\varkappa_2\right), \tag{30}$$

where the corrections to the Rabi formula read

$$\varkappa_1 = \delta^2 \frac{\pi^2 - 12(\ln 2)^2}{6}, \tag{31a}$$

$$\varkappa_2 = \frac{\beta}{2} \ln 2. \tag{31b}$$

These terms are positive and small compared to the respective leading terms: $\varkappa_1 \sim O(\tau^2)$ and $\varkappa_2 \sim O(\tau)$. The term $\varkappa_1$ describes the reduction of the oscillation amplitude due to the finite coupling rise time; it depends on the detuning only. The term $\varkappa_2$ describes the decrease of the oscillation frequency. These features are indeed observed in Figs. 2 and 4, which show that the features remain valid even outside the considered regime $\tau \to 0$. We note that the nonvanishing transition probability feature cannot be retrieved in the limit $\tau \to 0$ because it is characteristic of asymmetric pulses, whereas in the limit $\tau \to 0$ the tanh pulse becomes symmetric.

B. Slow rise: Shark model limit

In the opposite limit to that in the preceding section,

$$\tau \to \infty, \tag{32}$$

the coupling rises so slowly that the tanh function is nearly linear throughout the pulse duration: $\xi = \tanh(t/\tau) \approx t/\tau$. Then the tanh model reduces to the shark model,

$$\Omega(t) = \begin{cases} 0 & (t < 0,\ t > T), \\ \Omega_0 t/\tau & (0 \leqq t \leqq T), \end{cases} \tag{33}$$

which has been solved in a fashion similar to the present model [19]: after a $\pi/4$ rotation of the basis the Schrödinger equation was solved in terms of Weber's parabolic cylinder function $D_a(z)$ because in the rotated basis, the shark model turns into the Landau-Zener-Stückelberg-Majorana model [19,25]. Therefore we expect that in the limit (32) the Legendre functions in the tanh model should reduce to the Weber functions of the shark model. We verify these expectations rigorously in the Appendix.

IV. DISCUSSION AND CONCLUSIONS

In this paper, we have derived an exactly solvable time-dependent model of a two-state quantum system driven by a pulse of hyperbolic-tangent shape and constant detuning. This model resembles the famous Rabi model, but unlike the latter, the tanh model exhibits a gradual, rather than sudden, rise of the coupling. We have calculated the exact propagator in terms of associated Legendre functions. We have examined the limit when the Rabi and tanh models coalesce: the limit of fast rising of the tanh pulse. We have derived the corrections to the Rabi formula due to the finite rise time of the coupling, and we have found that for the tanh pulse both the amplitude and the frequency of the Rabi oscillations are reduced. In the limit of slow coupling rise, the tanh model reduces to the linear (shark) model; we have verified that our expressions for the propagator elements reduce to the ones for the shark model, which are expressed in terms of Weber's parabolic cylinder function. An interesting feature of the tanh model is that the transition probability does not vanish exactly, except in the trivial cases of vanishing pulse area or detuning; in other words, a two-state system excited by a tanh pulse cannot return to its initial state upon the completion of the pulse. We have attributed this feature to the asymmetry of the driving pulse.

Besides the general importance of exactly solvable time-dependent models of two-state quantum systems, the tanh pulse shape is of interest in some real experimental situations. For example, the rising edge of the rf field produced by a suddenly turned on rf generator has a shape very close to the tanh profile. The results presented in this paper allow one to describe more accurately the excitation produced in such situations. Moreover, our results make it possible to estimate the accuracy of the assumption of a rectangular pulse profile and therefore the conditions for the applicability of this assumption.

We point out that the tanh model assumes a sudden fall of the pulse, and hence it cannot describe a finite turn-off time. If this fall is fast, i.e., if the fall time is much shorter than the rise time, the tanh model can still be used to describe the postpulse excitation with high accuracy. We note that it is possible to describe analytically an exponential, rather than sudden, fall of the pulse. The solution for the exponential part, as in the Demkov model [15], is expressed in terms of Bessel functions [22]. The overall propagator then would be given by a product of our present propagator (19), expressed by associated Legendre functions, and another propagator for the exponential turn-off, expressed by Bessel functions. Although it is possible to write down the overall solution, it is far too cumbersome to be of practical use.

ACKNOWLEDGMENTS

This work has been supported by the EC Seventh Framework Programme under Grant Agreement No. 270843 (iQIT) and the Alexander-von-Humboldt Foundation.

APPENDIX: DERIVATION OF THE SHARK MODEL IN THE LIMIT $\tau \to \infty$

In order to verify that in the limit (32) the tanh model (3) reduces to the shark model (33), we first note that for fixed Ω and Δ, the variables α, β, and δ all tend to infinity in the limit (32),

$$\alpha \to \infty, \quad \beta \to \infty, \quad \delta \to \infty. \tag{A1}$$

Next, we use the representation of the associated Legendre functions in terms of the hypergeometric function [21],

$$\begin{aligned} P_\mu^\nu(\xi) = 2^\nu \sqrt{\pi}(1-\xi^2)^{-\nu/2} \Bigg[& \frac{1}{\Gamma\left(\frac{1}{2} - \frac{\mu+\nu}{2}\right)\Gamma\left(1 + \frac{\mu-\nu}{2}\right)} {}_2F_1\left(\frac{1}{2} + \frac{\mu-\nu}{2}, -\frac{\mu+\nu}{2}; \frac{1}{2}; \xi^2\right) \\ & - \frac{2\xi^2}{\Gamma\left(-\frac{\mu+\nu}{2}\right)\Gamma\left(\frac{1}{2} + \frac{\mu-\nu}{2}\right)} {}_2F_1\left(\frac{1}{2} - \frac{\mu+\nu}{2}, 1 + \frac{\mu-\nu}{2}; \frac{3}{2}; \xi^2\right) \Bigg], \end{aligned} \tag{A2a}$$

$$Q_\mu^\nu(\xi) = 2^\nu\sqrt{\pi}(1-\xi^2)^{-\nu/2}\left[\frac{\cos\frac{\pi(\mu+\nu)}{2}\Gamma\left(1+\frac{\mu+\nu}{2}\right)}{\Gamma\left(\frac{1}{2}+\frac{\mu-\nu}{2}\right)}\xi\ {}_2F_1\left(\frac{1}{2}-\frac{\mu+\nu}{2},1+\frac{\mu-\nu}{2};\frac{3}{2};\xi^2\right)\right.$$
$$\left.-\frac{\sin\frac{\pi(\mu+\nu)}{2}\Gamma\left(\frac{1}{2}+\frac{\mu+\nu}{2}\right)}{2\Gamma\left(1+\frac{\mu-\nu}{2}\right)}\ {}_2F_1\left(-\frac{\mu+\nu}{2},\frac{1}{2}+\frac{\mu-\nu}{2};\frac{1}{2};\xi^2\right)\right]. \quad \text{(A2b)}$$

Now we substitute Eq. (17) and the two equations above in Eq. (18). After some simplifications we obtain

$$V_{11} = (1-\xi^2)^{-\nu/2}\ {}_2F_1\left(\frac{1}{2}+\frac{\mu-\nu}{2},-\frac{\mu+\nu}{2};\frac{1}{2};\xi^2\right), \quad \text{(A3)}$$

where we have used several well-known properties of Euler's gamma function [21],

$$\Gamma(z+1) = z\Gamma(z), \quad \text{(A4a)}$$

$$\Gamma(z)\Gamma(1-z) = \frac{\pi}{\sin(\pi z)}, \quad \text{(A4b)}$$

$$\Gamma(z)\Gamma(z+\tfrac{1}{2}) = 2^{1-2z}\sqrt{\pi}\,\Gamma(2z). \quad \text{(A4c)}$$

Expression (A3) is *exact*. Now we apply conditions (32) and (A1). In this limit, we have $\xi \approx t/\tau \to 0$, $|\nu| \to \infty$, and $|\mu| \to \infty$. Hence, we can use the relations [21]

$$\lim_{|p|\to\infty}\left(1+\frac{z}{p}\right)^p = e^z, \quad \text{(A5a)}$$

$$\lim_{|p|\to\infty}\ {}_2F_1\left(a,p;c;\frac{z}{p}\right) = {}_1F_1(a;c;z), \quad \text{(A5b)}$$

where ${}_1F_1(a;c;z)$ is the confluent hypergeometric function. We find

$$\lim_{\tau\to\infty} V_{11} = e^{\nu\xi^2/2}\ {}_1F_1\left(\frac{1}{2}+\frac{\mu-\nu}{2};\frac{1}{2};-\frac{\mu+\nu}{2}\xi^2\right) \quad \text{(A6a)}$$
$$= e^{-\mu\xi^2/2}\ {}_1F_1\left(\frac{\nu-\mu}{2};\frac{1}{2};\frac{\mu+\nu}{2}\xi^2\right), \quad \text{(A6b)}$$

where the relation ${}_1F_1(a;b;z) = e^z\ {}_1F_1(b-a;b;-z)$ was used in the latter transformation.

Formula (A6b) can be expressed in terms of Weber's parabolic cylinder function $D_a(z)$. To this end, we use the definition of Weber's function [21],

$$D_a(z) = 2^{a/2}\sqrt{\pi}\,e^{-z^2/4}\left[\frac{1}{\Gamma\left(\frac{1-a}{2}\right)}{}_1F_1\left(-\frac{a}{2};\frac{1}{2};\frac{z^2}{2}\right)\right.$$
$$\left.-\frac{z\sqrt{2}}{\Gamma(-\frac{a}{2})}{}_1F_1\left(\frac{1-a}{2};\frac{3}{2};\frac{z^2}{2}\right)\right]. \quad \text{(A7)}$$

We find that

$${}_1F_1\left(-\frac{a}{2};\frac{1}{2};\frac{z^2}{2}\right) = \frac{\Gamma\left(\frac{1-a}{2}\right)e^{z^2/4}}{\sqrt{\pi}\,2^{1+a/2}}[D_a(-z)+D_a(z)], \quad \text{(A8a)}$$

$${}_1F_1\left(\frac{1-a}{2};\frac{3}{2};\frac{z^2}{2}\right) = \frac{\Gamma\left(-\frac{a}{2}\right)e^{z^2/4}}{\sqrt{2\pi}\,2^{1+a/2}z}[D_a(-z)-D_a(z)]. \quad \text{(A8b)}$$

We set $t = T$, $z^2 = (\mu+\nu)\xi^2 \approx 2i\alpha T^2/\tau^2 = i\gamma^2T^2$, and $a = \mu-\nu \approx -i\delta^2/(2\alpha) = -i\lambda^2$, where we have assumed that $\alpha \gg \delta$ and we have set $\gamma = \sqrt{2\alpha}/\tau$ and $\lambda = \delta/\sqrt{2\alpha}$. We substitute Eq. (A8a) in Eq. (A6b) and obtain

$$\lim_{\tau\to\infty} V_{11} = \frac{\Gamma(1+i\lambda^2)D_{-1-i\lambda^2}(0)}{\sqrt{2\pi}}$$
$$\times[D_{-i\lambda^2}(\gamma Te^{i\pi/4}) + D_{-i\lambda^2}(-\gamma Te^{i\pi/4})], \quad \text{(A9)}$$

where we have used relation (A4c) and [21]

$$D_a(0) = \frac{2^{a/2}\sqrt{\pi}}{\Gamma\left(\frac{1-a}{2}\right)}. \quad \text{(A10)}$$

Equation (A9) coincides with Eq. (7a) of Ref. [19], with an appropriate change of notation.

In a similar fashion one can derive $\lim_{\tau\to\infty} V_{12}$.

We conclude that in the limit of infinitely slow rise of the coupling, $\tau \to \infty$, the solution for the tanh model reduces to the one for the shark model [19], as must be the case.

[1] B. W. Shore, *The Theory of Coherent Atomic Excitation* (Wiley, New York, 1990).
[2] I. I. Rabi, Phys. Rev. **51**, 652 (1937).
[3] L. D. Landau, Phys. Z. Sowjetunion **2**, 46 (1932).
[4] C. Zener, Proc. R. Soc. London, Ser. A **137**, 696 (1932).
[5] E. C. G. Stückelberg, Helv. Phys. Acta **5**, 369 (1932).
[6] E. Majorana, Nuovo Cimento **9**, 43 (1932).
[7] N. Rosen and C. Zener, Phys. Rev. **40**, 502 (1932).
[8] L. Allen and J. H. Eberly, *Optical Resonance and Two-Level Atoms* (Dover, New York, 1975).
[9] F. T. Hioe, Phys. Rev. A **30**, 2100 (1984).
[10] A. Bambini and P. R. Berman, Phys. Rev. A **23**, 2496 (1981).
[11] Y. N. Demkov and M. Kunike, Vestn. Leningr. Univ., Ser. 4, Fiz. Khim. **16**, 39 (1969).
[12] F. T. Hioe and C. E. Carroll, Phys. Rev. A **32**, 1541 (1985).
[13] J. Zakrzewski, Phys. Rev. A **32**, 3748 (1985).
[14] K.-A. Suominen and B. M. Garraway, Phys. Rev. A **45**, 374 (1992).
[15] Y. N. Demkov, Sov. Phys. JETP **18**, 138 (1964).
[16] E. E. Nikitin, Opt. Spectrosc. **13**, 431 (1962); Adv. Quantum Chem. **5**, 135 (1970).
[17] C. E. Carroll and F. T. Hioe, J. Phys. A **19**, 3579 (1986).

[18] E. Barnes and S. Das Sarma, Phys. Rev. Lett. **109**, 060401 (2012).
[19] B. T. Torosov and N. V. Vitanov, J. Phys. A **41**, 155309 (2008).
[20] D. Schraft (private communication).
[21] http://functions.wolfram.com.
[22] N. V. Vitanov and P. L. Knight, J. Phys. B **28**, 1905 (1995).
[23] N. V. Vitanov, J. Phys. B **27**, 1351 (1994).
[24] N. V. Vitanov, J. Phys. B **28**, L19 (1995).
[25] N. V. Vitanov and B. M. Garraway, Phys. Rev. A **53**, 4288 (1996); **54**, 5458(E) (1996).